# Comparison of trimuon production mechanisms

C. H. Albright*
*Fermi National Accelerator Laboratory, Batavia, Illinois 60510*

J. Smith
*Institute for Theoretical Physics, State University of New York at Stony Brook, Stony Brook, New York 11794*

J. A. M. Vermaseren
*Department of Physics, Purdue University, West Lafayette, Indiana 47907*
(Received 30 January 1978)

We compare the predictions of six models for neutrino (and antineutrino) production of trimuon events. In particular, results are given for models based on heavy-charged-lepton decays, heavy-neutral-lepton decays together with heavy-quark decays, diffractive production and decay of heavy-quark pairs, heavy-quark cascade decays, the decays of Higgs mesons, and the radiative production of muon pairs. Our comparison should help to unravel the sources of the trimuon events detected at Fermilab and CERN. We also examine the probability of explaining the so-called superevents in which the muons are extremely energetic.

## I. INTRODUCTION

In the past year, observation of events with three muons in the final state has been reported by several experimental groups, using both narrow- and wide-band neutrino and antineutrino beams. In particular, by summer 1977 two events were found by the Caltech-Fermilab (CF) group,[1] thirteen events were recorded by the Fermilab-Harvard-Pennsylvania-Rutgers-Wisconsin (FHPRW) collaboration,[2] and three were detected by the CERN-Dortmund-Heidelberg-Saclay (CDHS) group.[3] At the time of this writing, all three experimental groups are continuing to take more data and have reportedly accumulated many more trimuon events, as well as two tetramuon events.[4]

While some of these events probably arise from prompt pion and kaon decay backgrounds, at least two "super" events have been found[2] which most certainly do not arise from this mechanism. For these events, the observed muon energies are large: (157, 32, and 47 GeV) and (96, 73, and 83 GeV), while the observed hadron energies are small ($E_{\rm had} = 13$ GeV) and ($E_{\rm had} \lesssim 30$ GeV), respectively.

Numerous models have been proposed in the literature to explain the trimuon events: heavy-lepton cascade decay,[5,6] simultaneous heavy-lepton and heavy-quark decays,[7,8] heavy-quark pair production and decay,[9,10] heavy-quark cascade decay,[11] Higgs-boson production and decay,[12] and, finally, production of a muon pair by radiation off the muon and quark lines.[13,14] Unfortunately, it is difficult to compare the model predictions directly, since the authors involved have not always made the same detailed tests for these models. In this paper we report on a systematic study of all these models and present some of the most critical tests for the viability of each model.

We have tried to make this paper rather brief and have avoided any discussion of incorporating the heavy leptons and heavy quarks into gauge-theory models. Many papers already exist on this subject.[15] Since the rates for trimuon production are still unclear, it is more profitable to discuss characteristic distributions for each of the classes mentioned above. We therefore only give a short summary of the models in Sec. II, leaving out details which can be found in published papers. However, in two cases, namely the heavy-quark pair production and decay and the heavy-quark cascade decay, our models differ from those discussed previously, so some additonal information is given.

The results presented in Sec. III are flux-averaged with the quadrupole-triplet wide-band spectrum used by the FHPRW group. We have examined the effects of using a narrow-band spectrum but do not find that this changes our conclusions. There are many correlations which can be measured in the trimuon events, so it should be rather easy to distinguish between classes of models once a sufficient number of events is measured. Note that it is always possible to make slight changes in the predictions of each model by varying the parameters, but there are significant differences between the classes of models. In the event that several sources are responsible for the trimuon events, the comparison with theoretical models will be more difficult.

In Sec. IV we give a short summary of our results. Also, we make some comments on the relative sizes of event rates for dimuon, trimuon, and tetramuon production in neutrino and antineu-

trino beams. In particular, the presence or absence of a $\mu^-\mu^-$ signal in neutrino interactions is extremely important in furthering our understanding of the physics behind trimuon phenomena. Bubble-chamber data on multilepton events containing electrons and/or positrons will also be very useful. Model-dependent limits on the masses of charged heavy leptons have already been presented by the BNL-Columbia collaboration.[16]

## II. PROPOSED MODELS

We sketch here briefly the models which we wish to compare. Further details can be found in the listed references. In general, the models can be divided into two classes, namely, those models which involve new quarks or leptons, and those that do not. In the latter category one can envisage the production of muon pairs (from trivial or nontrivial sources) in regular neutrino events. For instance, the radiative production of muon pairs or the production and decay of vector mesons will yield trimuon events. If these types of mechanisms are responsible for the trimuon events seen by the FHPRW and CDHS groups, then one does not expect to see any genuine same-sign dimuon signal, so the $\mu^-\mu^-$ event rate will be due to misidentified trimuons and will be much smaller than the $\mu^-\mu^-\mu^+$ event rate. The production of a Higgs scalar meson followed by its decay $H \to \mu^+\mu^-$ is another example (albeit academic) of this type.

The class of models which explain the trimuon events by invoking the production and decay of new heavy leptons and/or new heavy quarks has the feature that the multilepton event rates are controlled by the branching ratios for the heavy-lepton and/or heavy-quark decays. Assuming that the semileptonic decays of these new leptons or hadrons (which contain the new quarks) are suppressed compared to their hadronic decays, we expect to find a pattern in the multilepton decay rates. The $\mu^-\mu^-$ rate should be larger than the $\mu^-\mu^-\mu^+$, which in turn is larger than the $\mu^-\mu^-\mu^+\mu^+$, etc. This pattern is still expected to hold, even when events containing electrons and positrons are included and misidentified as muonic events. We also already know that there is no strong $\mu^-\mu^+\mu^+$ signal which imposes restrictions on the kind of decay chains allowed. Hence the identification of a large $\mu^-\mu^-$ or $\mu^-e^-$ event rate is necessary for establishing the validity of these models. Note that we exclude any discussion of opposite-sign dimuon pairs because they will be hard to observe in the presence of single-charm production and decay. An analysis of $\mu^-\mu^+$ signals will be reported later.

The models we consider fall into both classes. The first two only allow the production of muon pairs, while the other four are representative of different types of heavy-hadron or heavy-lepton models. The multimuon event rates for the latter four models are uncertain until specific gauge theories are constructed. However, the experimental rate is also uncertain and that is why we concentrate on distributions to distinguish one model from another.

### A. Dalitz production of muon pairs

In this model, a virtual photon is radiated from the charged muon and quark lines, and converts into a real muon pair, i. e.,

$$\nu_\mu + N \to \mu^- + \text{“}\gamma\text{”} + X, \qquad \gamma \to \mu^+\mu^- . \tag{2.1}$$

To maintain gauge invariance in the calculation, all the diagrams shown in Fig. 1 must be considered. In addition, the two identical muons should be antisymmetrized. Two of the authors (J.S. and J.V.) have reported results for this model in a recent paper,[13] to which we refer the reader for details. We discuss some of the important results in Sec. III. Note that the *electromagnetic* production of real vector mesons $\rho$, $\psi$, $\Upsilon$ etc., has been discussed by Godbole,[12] and her conclusion is that the rate is too small to account for the experimental value for trimuon production.

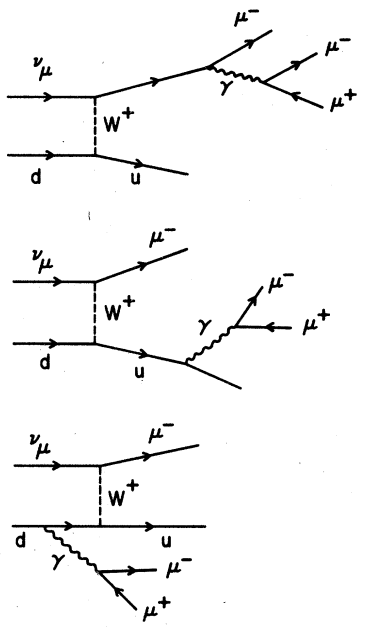


FIG. 1. Feynman diagrams for the radiative production of muon pairs.

If this radiative mechanism is the only one contributing to trimuon production, then we do not expect to see genuine dimuons or tetramuons. Hence, $\mu^-\mu^-$ events will only occur if the $\mu^+$ does not survive the energy cut and its rate will be approximately one order of magnitude smaller than the trimuon production rate. The $\mu^-\mu^+$ mode will occur at the same level as the $\mu^-\mu^-$, but will be buried in the opposite-sign dimuon signal from the decays of charmed particles. Tetramuon events must arise from some background process such as $\pi$ or $K$ decay in flight. Events containing $\mu^-e^-e^+$ particles will be seen in bubble-chamber exposures with an $e^-e^+$ invariant mass larger than that of the $\pi^0$. However, $\mu^-e^-$ events will be extremely rare.

### B. Higgs-boson production and decay

In this process, a scalar Higgs particle can be emitted from the muon, quark, or intermediate-vector-boson lines. Since the effective coupling is proportional to the mass of the field which emits the Higgs particle, the emission from the $W$-boson line is by far the most important. This diagram is illustrated in Fig. 2. Godbole[12] has investigated this mechanism for Higgs-boson masses in the range 3 to 7 GeV/$c^2$. We only consider the decay mode of the Higgs particle into a dimuon pair. Hadronic decays involving charmed particles will also lead to events with a $\mu^+\mu^-$ pair, but the invariant mass of the pair will not peak at a fixed value. Hence, we consider the reaction

$$\begin{aligned} \nu_\mu + N &\to \mu^- + H + X \\ &\qquad \searrow \mu^+\mu^-, \end{aligned} \tag{2.2}$$

where $H$ stands for the Higgs particle, whose mass we take to be 4 GeV/$c^2$.

Our motivation for including this particular mechanism is to understand its kinematic features. We are well aware that the two-body branching ratio for $H \to \mu^+\mu^-$ will be extremely small and, therefore, $B$ will be much too small to account for the trimuon event rate. However, reaction (2.2) is an example of the production of a dimuon pair with large invariant mass as compared to model A, which involves the production of a dimuon pair with small invariant mass. If reaction (2.2) is to be the explanation of the trimuon events, then we would expect a much lower rate for $\mu^-\mu^-$ events and no genuine tetramuon events. Bubble-chamber experiments would never see $\mu^-e^-e^+$ events because the branching ratio for $H \to e^+e^-$ is proportional to the lepton mass and therefore exceedingly small.

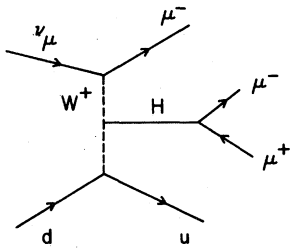


FIG. 2. Feynman diagram for the production and decay of a Higgs boson.

### C. Hadron (quark) cascade

In this model one assumes that a charge $\frac{2}{3}$ $t$ quark is excited in neutrino interactions, which subsequently decays into lighter-mass quarks. Soni[11] has considered both the quark chain $t \to b \to u$ and the chain $t \to b \to \tau$, where $\tau$ is the heavy lepton discovered by Perl *et al.*[17] Barnett and Chang[7] have investigated the decay $t \to \mu^+ + M^0 + X$, where $M^0$ is a neutral heavy lepton which decays into $\mu^- + X$. We investigate the decay chain

$$\begin{aligned} \nu_\mu + N &\to \mu^- + T + X \\ &\qquad \searrow B + X' \\ &\qquad\quad \searrow C + \mu^- + \bar{\nu}_\mu \\ &\qquad\qquad \searrow S + \nu_\mu + \mu^+ \end{aligned} \tag{2.3}$$

as illustrated in Fig. 3, where $T$, $B$, $C$, and $S$ refer to hadrons containing a $t$, $b$, $c$, or $s$ quark and $X, X'$ represent any other hadrons. The $\mu^+$ could instead be emitted in the $T$-$B$ transition, but there are no experimental indications of a strong $\mu^-\mu^+\mu^+$ signal, so we have to assume that the semileptonic decay width of $T \to B$ is suppressed compared to its nonleptonic decay width. As we expect the more massive quarks to have many hadronic decay channels, the assumption is not unreasonable.

This model allows the emission of zero to four leptons, with increasing powers of the leptonic branching ratio which emphasizes the importance of knowing the event rates for multilepton signals. In the absence of detailed information on these rates, we choose the chain in (2.3) for the purpose of illustrating the typical distributions expected

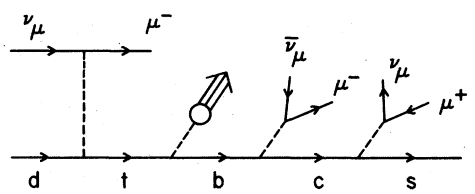


FIG. 3. Feynman diagram for the heavy-quark cascade decay.

from a hadronic decay chain. The quark transition $d \to t$ involved in the production process is assumed to be right-handed, as are the $t \to b$ and $b \to c$ transitions. We take the quark masses $m_t$, $m_b$, $m_c$, and $m_s$ equal to 7.5, 4.75, 1.5, and 0.5 GeV/$c^2$, respectively.

### D. Diffractive production of heavy-quark pairs

Bletzacker and Nieh[9] have considered associated production of charm at small $x$ as the mechanism responsible for trimuon production. From charge conservation it is clear that $c\bar{c}$ pairs cannot be produced in a normal diffractive way (via Pomeron exchange) from a charged $W$ boson. Production of $c\bar{c}$ pairs at intermediate $x$ has been discussed by Goldberg[10] in the framework of quantum chromodynamics. We consider here the diffractive production of a $c\bar{b}$ pair from a $W^+$ boson and assume that a gluon is exchanged between one of the quarks and the hadron vertex. This is shown in Fig. 4 for the reaction

$$\begin{aligned} \nu_\mu + N &\to \mu^- + C + \bar{B} + X \\ &\quad\searrow\ \bar{C} + X' \\ &\quad\qquad\searrow\ \bar{S} + \mu^- + \bar{\nu}_\mu \\ &\quad\searrow\ S + \nu_\mu + \mu^+ \,. \end{aligned} \tag{2.4}$$

Alternatively, a $\mu^+$ could be emitted in the $\bar{b} \to \bar{c}$ transition, but this would imply that many $\mu^-\mu^+\mu^+$ events would be observed as well as $\mu^-\mu^-\mu^+$ events, which does not appear to be the case. In principle, four muons can arise from this diffractive process, and the event rates are proportional to the product of the semileptonic decay rates. The choice of a nonleptonic $\bar{b} \to \bar{c}$ transition is in agreement with the choice in the previous model. We have used the same values for the quark masses as given above.

Thus our model is very similar in spirit, and in computational details, to the Bletzacker-Nieh model. We assume the production cross section to be determined by a structure function $F(x, y)$ given by

$$F(x,y) = \frac{Q^2}{(Q^2+4M_0^2)}\left(\frac{s-s_0}{s}\right)^3 e^{-10z'}\left[1+(1-y)^2\right] ,$$

where $x = Q^2/(2M\nu)$, $y = \nu/E$, $s = 2M\nu - Q^2 + M^2$, and $M$ is the nucleon mass. The threshold factor $s_0$, mass $M_0$, and $z'$ variable depend on the masses of the quarks. We have chose $M_0 = M_B - M$, $s_0 = [M + (m_c + m_b)]^2$, and $z' = [Q^2 + (m_c + m_b)^2]/(2M\nu)$, where $m_c$ and $m_b$ are the quark masses and $M_B = 5.5$ GeV/$c^2$ is the mass of the lightest $b$-flavored hadron.

### E. $M^0$ heavy-lepton, heavy-quark production

This type of mechanism for trimuon production was discussed previously by Barnett and Chang,[7] and by Barger *et al.*,[8] who assumed the simultaneous production of a neutral heavy lepton $M^0$ and a $b$ quark. The decay $b \to u$ occurs with the emission of a $\mu^-$. We assume that the dominant decay mode of the $b$ quark is semileptonic and involves the emission of a $c$ quark, namely,

$$\begin{aligned} \nu_\mu + N &\to M^0 + B + X \\ &\quad\searrow\ C + \mu^- + \bar{\nu}_\mu \\ &\quad\searrow\ \mu^- + \nu_\mu + \mu^+ \,, \end{aligned} \tag{2.5}$$

which is depicted in Fig. 5. In this process, four muons can be emitted if the charmed quark also decays leptonically. We assume that the mass of the $M^0$ is in the range 2–4 GeV/$c^2$, but we illustrate our results only for the 4-GeV/$c^2$ case, with $m_b = 4.75$ GeV/$c^2$ and $m_c = 1.5$ GeV/$c^2$. If the quark transition were taken to be $b \to c + X$ followed by $c \to s + \mu^+ + \bar{\nu}_\mu$, we would predict too many $\mu^-\mu^+\mu^+$ events, which is incompatible with the present experimental results.

### F. $M^-$ heavy-lepton cascade

In this process the trimuon events arise from the reaction

$$\begin{aligned} \nu_\mu + N &\to M^- + X \\ &\quad\searrow\ L^0 + \mu^- + \bar{\nu}_\mu \\ &\quad\searrow\ \mu^- + \nu_\mu + \mu^+ \end{aligned} \tag{2.6}$$

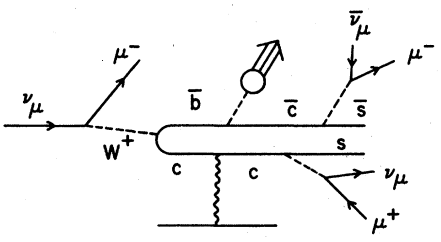


FIG. 4. Feynman diagram for the diffractive production and decay of a pair of heavy quarks.

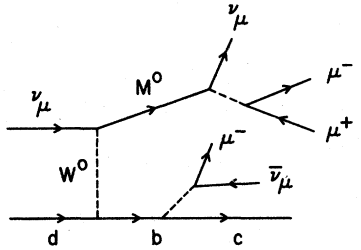


FIG. 5. Feynman diagram for the production and decay of a neutral heavy lepton and a heavy quark.

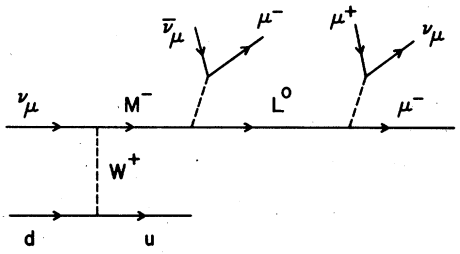


FIG. 6. Feynman diagram for the charged-heavy-lepton cascade decay.

illustrated in Fig. 6 and discussed in the literature at some length by the present authors[5] as well as by Barger et al.[6] Production of the $M^-$ can be accompanied by either light- or heavy-quark production based on the particular gauge model one wishes to consider. We illustrate our results in Sec. III for the case of a $d \to u$ transition at the hadron vertex. The mass of the $M^-$ is 8 GeV/$c^2$ and the mass of the $L^0$ is set equal to 4 GeV/$c^2$. Results for the light-to-heavy-quark transitions can be found in Ref. 5 and 18. The multimuon event rates for the chain (2.6) depend on the $M^-$ and $L^0$ semileptonic branching ratios. One expects the $\mu^-\mu^-$ event rate to be larger than that for the $\mu^-\mu^-\mu^+$. In Ref. 18 this question was examined in detail for one SU(3)×U(1) gauge model and the tetramuon event rate was calculated. Also, the consequences of misidentifying events containing electrons and/or positrons was studied together with the effects of the minimum energy cuts on the muons. The latter effect is important when many muons are emitted and causes a large number of tetramuon events to be classified as trimuon events.

## III. NUMERICAL COMPARISONS

In order to carry out numerical calculations, we adopt the parton-model formalism and use the slow-rescaling approach, where the scaling variable is

$$\xi_j = x + m_j^2/(2MEy) \tag{3.1}$$

in terms of $x = q^2/2M\nu$, $y = \nu/E$, and $m_j$, the mass of the heavy quark of type $j$. To treat the physical threshold correctly, we use $M_C = 2.25$ GeV/$c^2$ for the lightest charmed hadron, $M_B = 5.5$ GeV/$c^2$ for the lighest $b$-flavor hadron, and $M_T = 8.5$ GeV/$c^2$ for the $t$-flavor hadron, where we recall $m_c = 1.5$ GeV/$c^2$, $m_b = 4.75$ GeV/$c^2$, and $m_t = 7.5$ GeV/$c^2$ were chosen for the quark masses of the corresponding flavors.

To fold in the decay chains, it is necessary to make assumptions about the quark-parton-model fragmentation functions $D_j^k(z)$ which give the probability that a quark of type $j$ will convert into a hadron of type $k$, where $z = E_k/E_j$ is the ratio of the energy $E_k$ carried by the hadron compared to the maximum allowed value. While the pion fragmentation functions $D^\pi(z)$ are found to fall off like $D^\pi(z) \simeq (1-z)/z$, the functions are not anticipated to peak at $z = 0$ for heavier hadrons. In fact, studies of the mass effects by Odorico,[19] Suzuki,[20] and Bjorken[21] suggest that, to a fair approximation, we can set

$$\begin{aligned} D^C(z) &= 1.0 \\ D^B(z) &= \delta\left(z - \left(1 - \frac{M}{m_b}\right)\right) \\ D^T(z) &= \delta\left(z - \left(1 - \frac{M}{m_t}\right)\right), \end{aligned} \tag{3.2}$$

where $m_b$ and $m_t$ are the $b$ and $t$ quark masses and $M$ is the nucleon mass. For the values of the masses selected, the fractional energy distribution for the hadron from the $B$ quark peaks at $z \cong 0.8$, while that for the $T$ peaks at $z \cong 0.9$. In semileptonic decays of the hadrons, the muons can thus be emitted with relatively high energies.

We now proceed to give some distributions for the processes under consideration. It is impractical to publish all the possible correlations between the three muons and the final hadrons. We have studied them to select the most discriminating. In general, the single differential distributions which are the most helpful are the production cross sections, the energy distributions of the muons and hadrons, the invariant masses of the pairs, the transverse momenta perpendicular to the neutrino direction and to the plane containing the fast $\mu^-$ and the $\nu$, and the azimuthal correlations in the plane perpendicular to the neutrino beam. We distinguish the two negative muons by binning them into fast and slow according to their energy, and call $E_1 = E_{\mu^-,\,\mathrm{fast}}$, $E_2 = E_{\mu^-,\,\mathrm{slow}}$, and $E_3 = E_{\mu^+}$ in the usual way. All the distributions are given after weighting by the FHPRW quadrupole-triplet spectrum.

### A. Cross sections and threshold effects

The production cross sections for the six reactions we consider have different characteristics. For example, the threshold for the radiative process is very low, apart from the fact that the muons must be produced with sufficient energies to be detected ($E_\mu \gtrsim 4$ GeV). The other reactions have different thresholds depending on the masses of the particles involved. For the production of heavy leptons in particular, the threshold can be pushed relatively high if they are only produced in association with heavy quarks. Higgs-meson

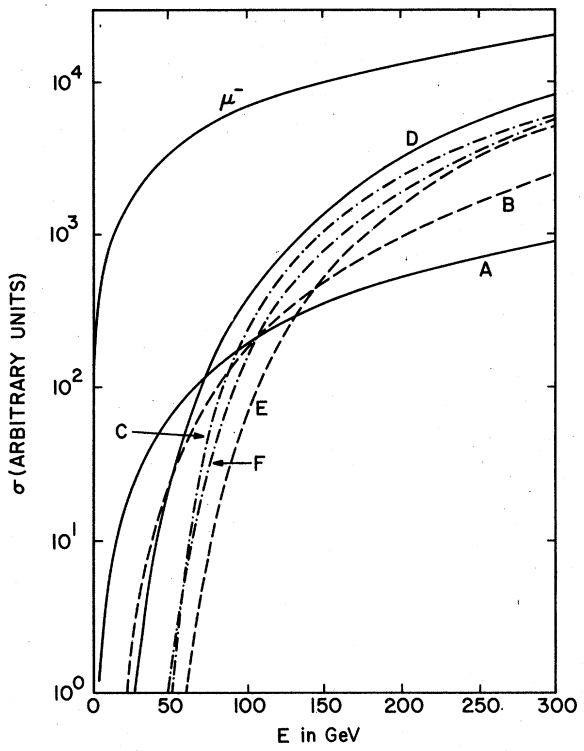


FIG. 7. Production cross sections for the six models considered in this paper. We use solid lines for the results of models A and D, dashed lines for models B and E, and dot-dashed lines for models C and F. The single-$\mu^-$ inclusive cross section is also shown for comparison.

masses are generally unknown and, for our choice of 4 GeV/$c^2$, the production threshold is lower than that for models C, D, E, and F. We illustrate these remarks by giving the energy dependences of the production cross sections in Fig. 7 for the masses chosen above. In order to distinguish more easily between the different models, we follow the convention that results from models A (radiative) and D (diffractive) are shown with solid lines, results from models B (Higgs) and E ($M^0$ hadron) are shown with dashed lines, and results from models C (hadron cascade) and F (lepton cascade) are shown with dot-dashed lines. In Fig. 7 we also show the regular single-muon inclusive cross section which rises linearly with the beam energy $E$. The cross sections have not been folded by the neutrino flux distribution. The radiative cross section has the lowest threshold and increases like $E \ln^2 E$ for large values of the beam energy. The cross sections for B and D increase with $E$ quadratically. All the other cross sections are asymptotically linear in $E$; however, because we have chosen large masses for the quarks and leptons, these asymptotes are only

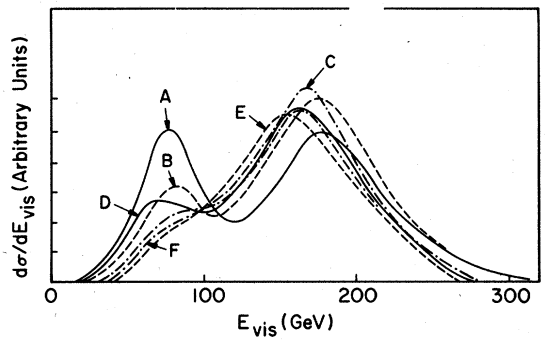


FIG. 8. $E_{\rm vis}$ distributions for the six models considered. The notation is the same as in Fig. 7.

reached beyond the energies attainable at Fermilab and CERN.

In Fig. 8 we show the visible energy distribution when the cross sections are folded by the FHPRW quadrupole-triplet wide-band spectrum. Note that the $E_{\rm vis}$ distributions for models C, D, E, and F are not the same as the $\sigma \times$ flux plots because there are always two neutrinos which carry away some energy. This systematically lowers the energies of the events and makes the reactions appear to have smaller thresholds. The present data from the FHPRW group consist of eleven $\mu^-\mu^-\mu^+$ events where all the muon energies are measured. However, the hadron energies are only known for four of the events, so the visible energy of the other events is larger than the sum of the three muon energies by an unknown amount. We give a histogram plot of the visible energies of the FHPRW data in Fig. 9 and cross hatch those events where the hadron energy is unknown. It is clear that the distribution of trimuon events versus the total visible energy will reflect both the threshold behavior and the asymptotic values of the cross sections. With a reasonable increase in statistics it will be possible to see if there is any hint of an energy threshold. However, a word of caution is necessary at this point. If heavy-lepton and/or heavy-quark models are the explanation of some of the trimuon events, there will be missing neutrinos,

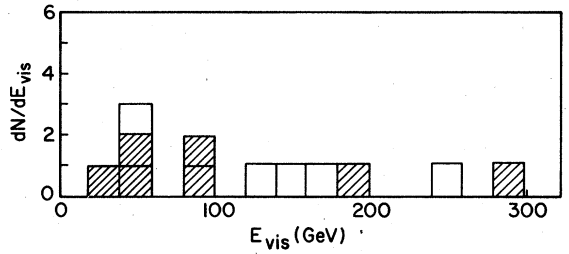


FIG. 9. Histograms of the visible energies for the FHPRW events. Those events which are hatched do not have a measured $E_{\rm had}$.

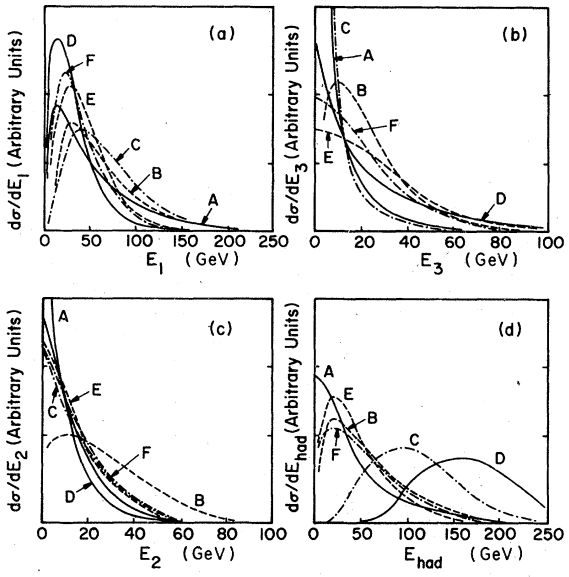


FIG. 10. Energy distributions for the six models. The notation is the same as in Fig. 7.

so the total energy in each event will only be accurately determined in a narrow-band dichromatic-beam experiment.

### B. Energy distributions

In Fig. 10, we show the energy distributions of the three muons for the models and the distributions in the hadron energies. Figure 11 gives the corresponding histograms of the FHPRW data. It is impractical to add all six theoretical predictions to the graphs with the data, so we present them separately. Our curves for the distributions are not scaled in any particular way as we have not tried to normalize the event rates. Clearly, the $\mu^+$ tends to be rather slow when it arises from the decay of a massive quark. The ordering of the two $\mu^-$ particles into $\mu^-_{\text{fast}}$ and $\mu^-_{\text{slow}}$ generally makes the slow $\mu^-$ have a lower average energy than the $\mu^+$. In most models, the slow $\mu^-$ and the $\mu^+$ have a reasonable probability that they will not escape the experimental minimum energy cut ($E_\mu \gtrsim 4$ GeV), so genuine trimuon events will therefore be registered as $\mu^-\mu^+$ or $\mu^-\mu^-$ events. The opposite-sign dimuon pairs may not stand out from the signal caused by the decays of charmed particles; however, the $\mu^-\mu^-$ events should be detected and will provide good evidence for/or against a particular model.

From Fig. 10 one sees that the hadronic energy distribution will help to differentiate between the models. The diffractive model (D) gives soft muons and a hard-hadron spectrum. Also, the hadronic-cascade model (C) is very effective in producing energetic hadrons accompanied by soft muons. The double differential distributions in the energies, to be presented later, show these features very clearly.

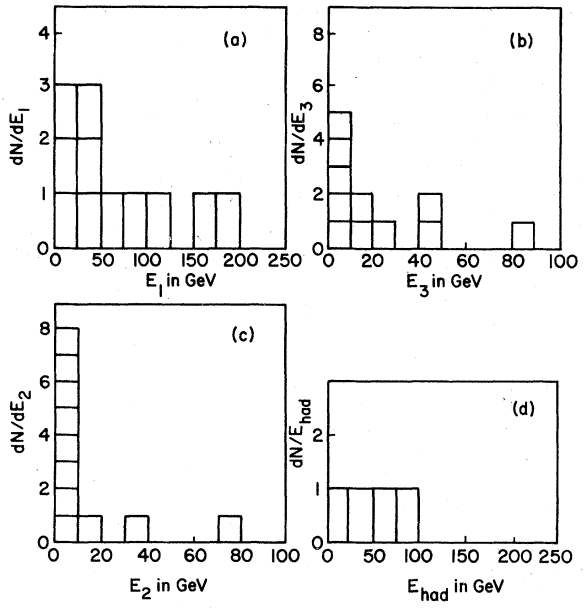


FIG. 11. Histograms of the energy distributions for the FHPRW events.

### C. Invariant-mass plots

The invariant-mass plots shown in Fig. 12 make precise the general features expected from qualitative arguments and should be compared with the data given in Fig. 13. When the muons are produced in heavy-lepton (or heavy-quark) decays, the $M_{123}$ distribution cannot be larger than the mass of the heaviest lepton (or particle carrying the quantum numbers of the quark). However, if the muons are produced in different decay chains, there is no corresponding limit on the trimuon invariant mass. Thus, if no events are found with masses larger than, say, 6 GeV/$c^2$, the $M^0$-hadron model as well as the Higgs particle model will probably have to be excluded as the only source of the trimuon events. The distributions in the invariant masses of the pairs also contain valuable information. Obviously, the $M_{23}$ invariant mass provides a decisive test of radiative versus nonradiative processes. The electromagnetic production shows a typical bremsstrahlung spectrum which is bounded at small masses by the sum of the masses of the two muons. In contrast, the Higgs boson case yields a dramatic peaking in the $M_{23}$ invariant mass (assuming a two-body decay into $\mu^+\mu^-$). This feature can be

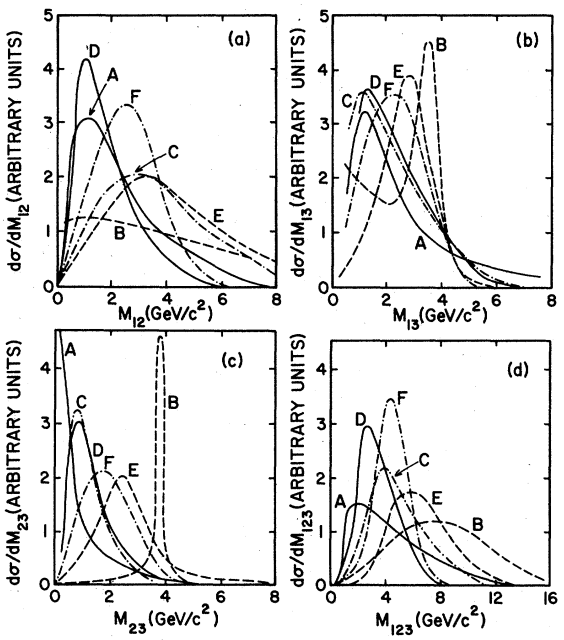


FIG. 12. Distributions in the invariant masses. The notation is the same as in Fig. 7.

exploited to bound the mass of the Higgs particle using models to calculate the branching ratio $H \to \mu^+\mu^-$.

### D. Transverse momenta

The transverse momenta perpendicular to the neutrino direction or perpendicular to the plane

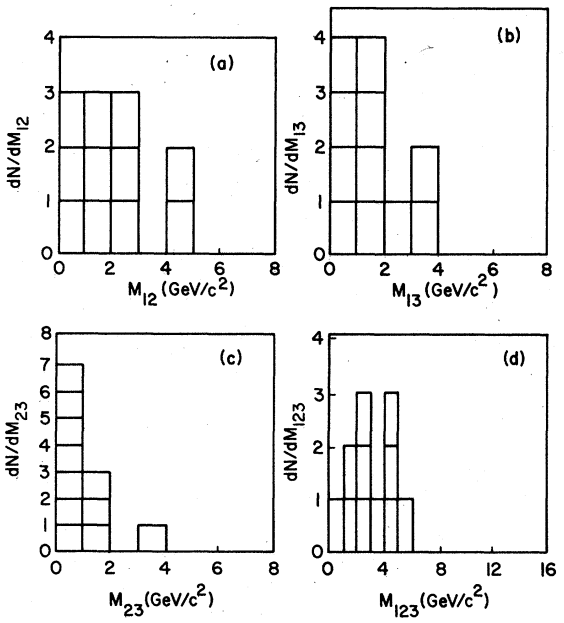


FIG. 13. Histograms of the invariant masses for the FHPRW events.

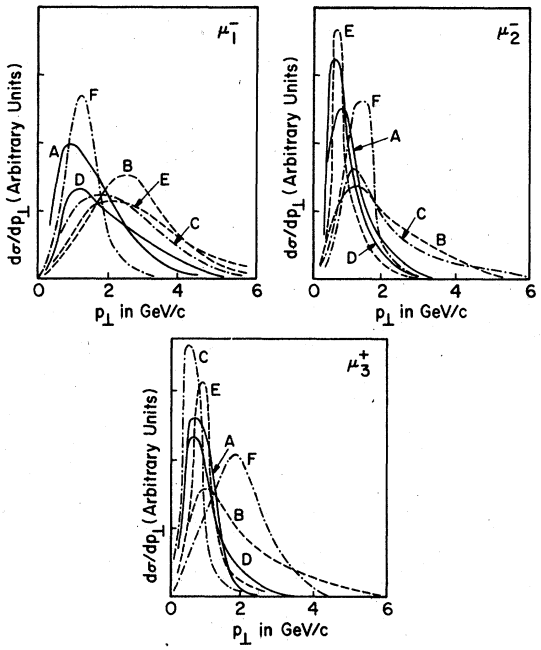


FIG. 14. Distributions in the transverse momenta perpendicular to the direction of the neutrino beam. The notation is the same as in Fig. 7.

containing the fast $\mu^-$ and the $W^+$ contains valuable information on whether the other muons are produced in a pointlike fashion. Both the hadronic-cascade and the leptonic-cascade mechanisms

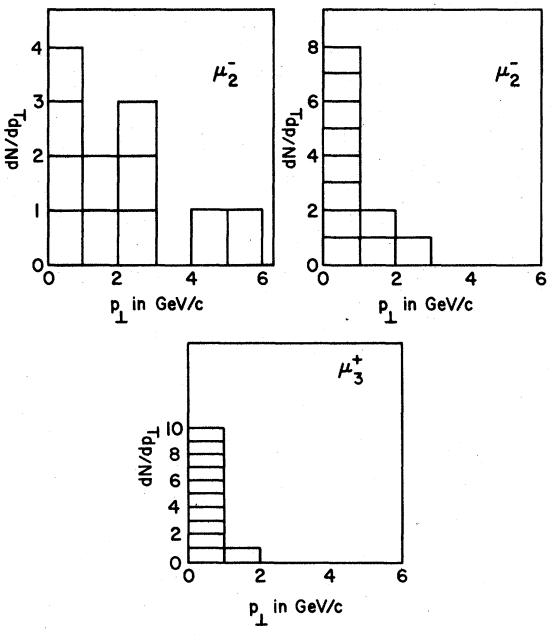


FIG. 15. Histograms of the transverse momenta perpendicular to the direction of the neutrino beam for the FHPRW events.

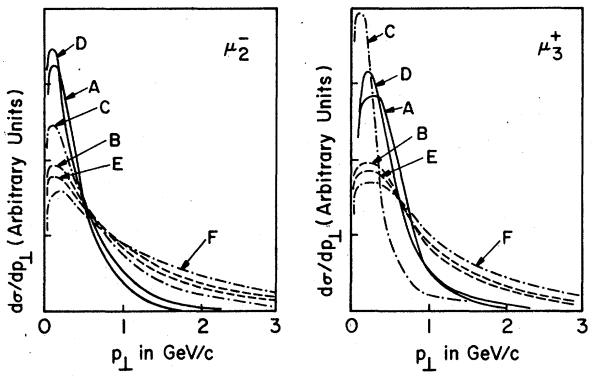


FIG. 16. Distributions in the transverse momenta of the slow $\mu^-$ and the $\mu^+$ perpendicular to the plane of the $\nu$ and the fast $\mu^-$. The notation is the same as in Fig. 7.

yield muons with large transverse momenta. In Fig. 14 we show the transverse-momentum spectra relative to the direction of the neutrino beam. The histograms showing the corresponding results for the FHPRW events are shown in Fig. 15. We complement this information by giving the theoretical transverse momenta of both the slow $\mu^-$ and the $\mu^+$ with respect to the plane containing the neutrino and the fast $\mu^-$ in Fig. 16. The corresponding data are shown in Fig. 17. The latter distributions are all peaked at rather low values of $p_\perp$.

### E. Azimuthal angles

Other key correlations in distinguishing between production mechanisms are the azimuthal angles between pairs of dimuon transverse momenta projected on the plane perpendicular to the neutrino beam. The results for the models discussed in the text are given in Fig. 18, while the data are shown in Fig. 19. The $\phi$ distributions are, unfortunately, rather difficult to measure accurately, so we must await more events before any firm

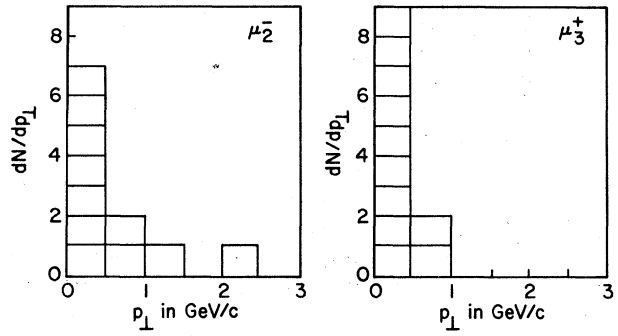


FIG. 17. Histograms of the transverse momenta of the slow $\mu^-$ and the $\mu^+$ perpendicular to the plane of the $\nu$ and the fast $\mu^-$ for the FHPRW events.

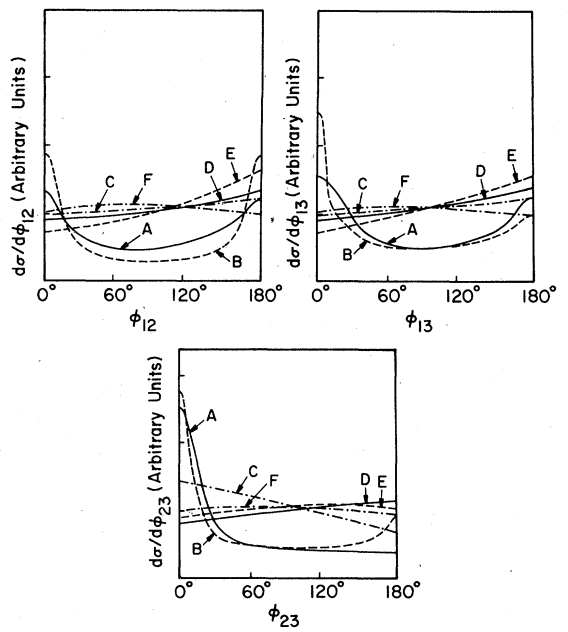


FIG. 18. Distributions in the azimuthal angles between the muons in the plane perpendicular to the direction of the neutrino beam. The notation is the same as in Fig. 7.

conclusions can be drawn.

The $\phi_{12}$ angle between the projections of the two negative muons contains valuable information on whether the second muon arises from the leptonic side of the interaction or the hadronic side. Had-

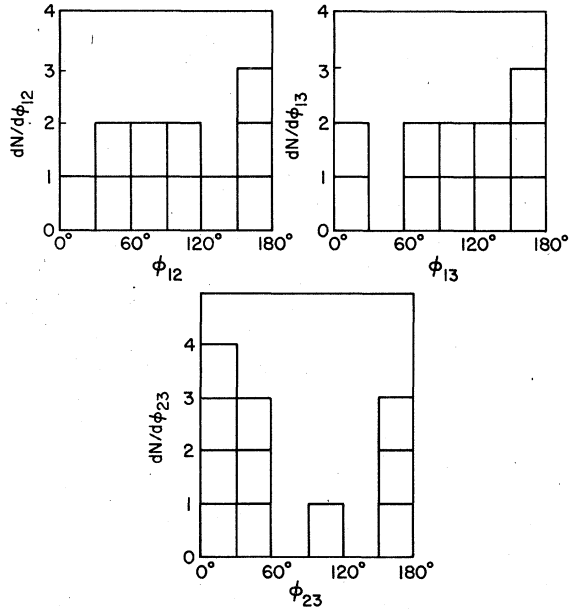


FIG. 19. Histograms of the azimuthal angles between the muons in the plane perpendicular to the direction of the neutrino beam for the FHPRW events.

ronic-cascade-decay models yield muons which are directed along the direction of the hadron jet, so $\phi_{12}$ peaks at 180°. This correlation is clearly present in the opposite-sign dimuon events arising from the production and decay of charmed particles.[22] The $\phi$ angles in the radiative process have more structure, which reflects the cancellation among the terms in the matrix element due to gauge invariance. The forward peaking is caused by radiation from the muon and the backward peaking is cuased by radiation from the hadrons (quarks).

### F. Double differential distributions

We have examined several double differential distributions. One plot we found to be very useful is a scatter plot of $E_1 - E_{\rm had}$ versus $E_2+E_3$. Rather than draw actual scatter plots, we present the same information by giving the number of events (normalized to approximately 1,000 events) in bins of 40 GeV versus 15 GeV in Figs. 20–25. This information also helps to evaluate the probability of explaining the extremely energetic events seen at Fermilab by the FHPRW group. These events have $E_1 - E_{\rm had}$ values of ~150 and ~70 GeV, while the $E_2+E_3$ values are ~75 and ~155GeV respectively. We have added the measured points to the scatter plots as dots (when the hadron energy is measured)

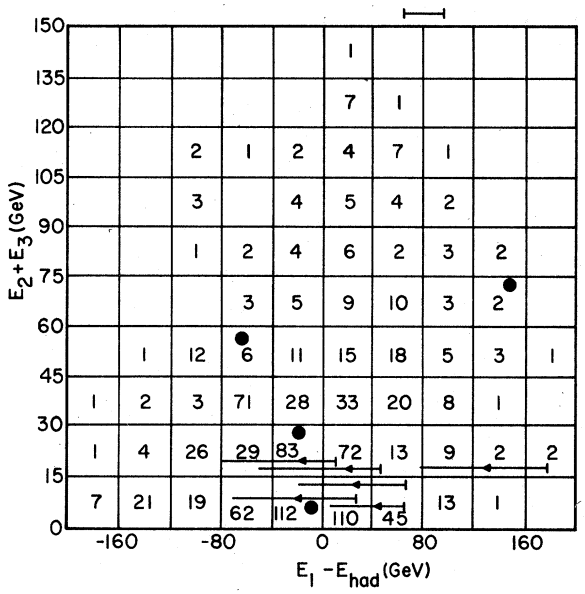


FIG. 20. Number of events in a two-dimensional scatter plot of $E_2+E_3$ versus $E_1-E_{\rm had}$ for model A (electromagnetic production). The total number of events is normalized to approximately 1000. The dots represent the FHPRW events where $E_{\rm had}$ is measured, and the lines represent the FHPRW events where $E_{\rm had}$ is not measured.

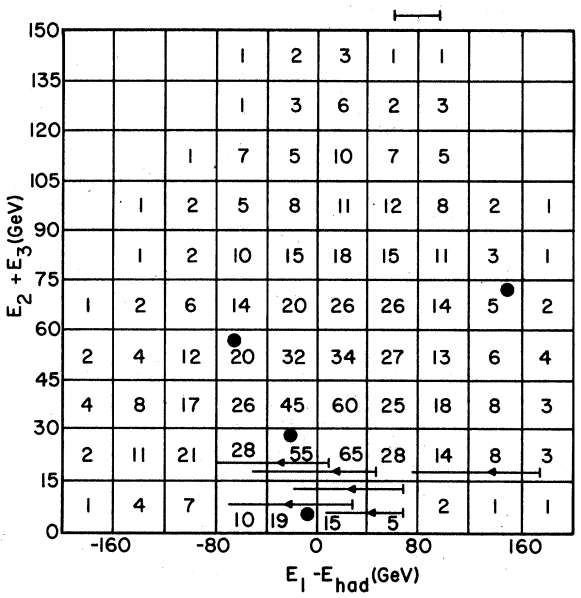


FIG. 21. Same as Fig. 20 for model B (Higgs-boson production).

and lines (when $E_{\rm had}$ is not known). In general, $E_{\rm had}$ cannot be too large; otherwise, the hadronic shower will punch through the iron in the FHPRW experiment and be detected.

In Fig. 20 we give the results for model A. Clearly, the probability of producing events with $E_2+E_3 \gtrsim 60$ GeV is very small. The situation is much better in the case of Higgs-boson production as illustrated in Fig. 21. Figure 22 shows the scatter

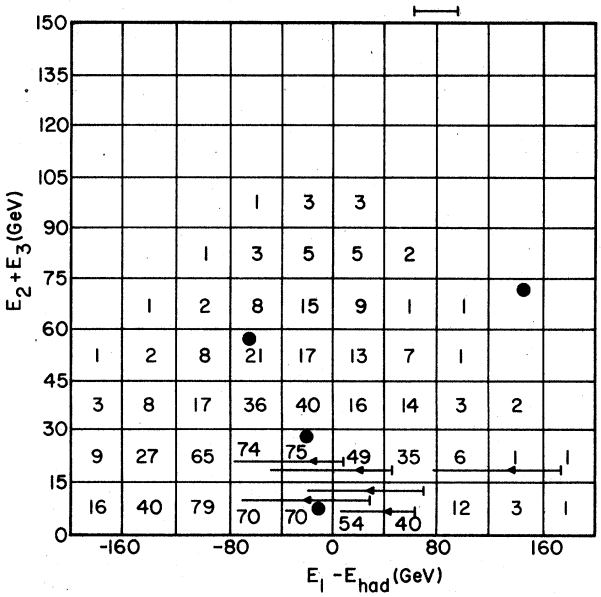


FIG. 22. Same as Fig. 20 for model C (hadron cascade).

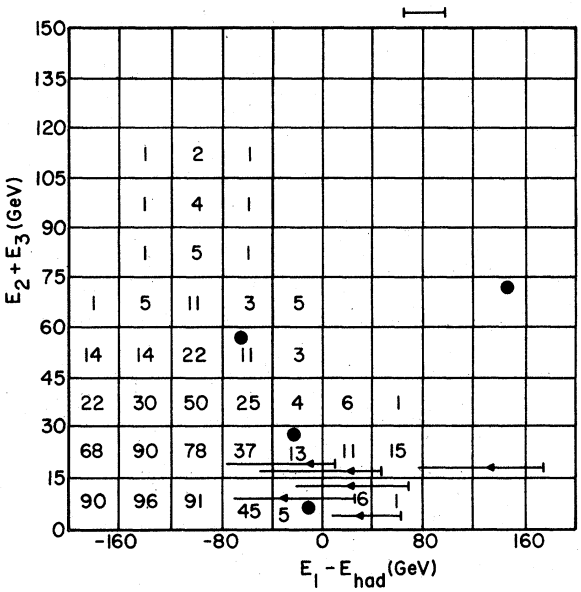


FIG. 23. Same as Fig. 20 for model D (diffractive production).

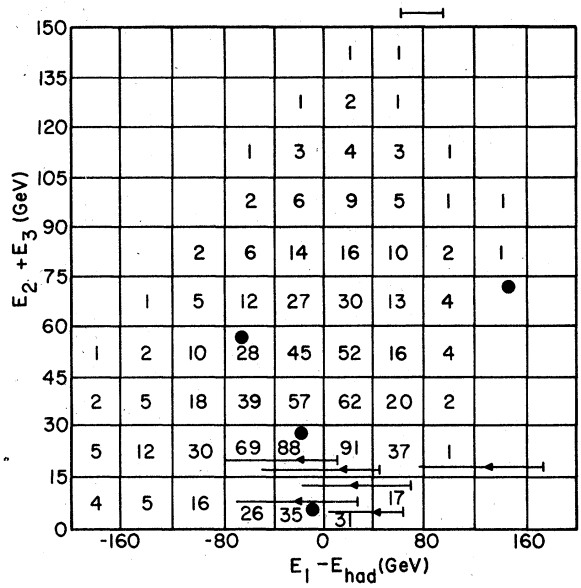


FIG. 25. Same as Fig. 20 for model F (heavy-lepton cascade).

plot for the hadron-cascade model, where both secondary muons are rather soft. In this model, $E_{had}$ tends to be larger than $E_1$, so most of the events fall in the region where $E_1 - E_{had}$ is negative. This latter feature is even more pronounced in the scatter plot for the diffractive model given in Fig. 23. However, if we turn to the $M^0$-hadron model, then the secondary muons tend to be almost as fast as the primary (i.e., fast) $\mu^-$ and the distribution of events changes dramatically. This

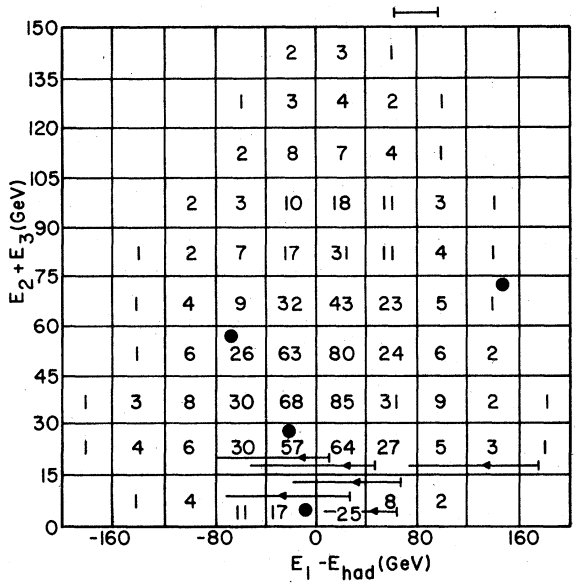


FIG. 24. Same as Fig. 20 for model E ($M^0$-hadron).

model has some events in the regions where the energetic events fall, but, again, the probability is very small. Finally, the results are given for the heavy-lepton-cascade model in Fig. 25. This model was constructed to give fast mons and one can obtain $E_2+E_3$ values as large as 70–80 GeV with a small probability.

The second correlation we present is that of $E_{had}$ versus the energy of the slowest muon $E_{slowest}$. The latter can have either charge. In the next series of plots from Figs. 26–31, we show this two-dimensional correlation for the models in bins of 10 GeV by 40 GeV and add the data points from the FHPRW experiment. The hadron-cascade model (Fig. 28) and the diffraction model (Fig. 29) clearly have different distributions of events from those of the other four models. Figures 26–31 are also helpful in assessing the probability of finding super events, but, unfortunately, $E_{had}$ is not known for event number 281-147196. However, the sum of the muon energies is already 260 GeV for this event, so $E_{had}$ is unlikely to be larger than 40 GeV. Clearly, it is very difficult to find any explanation of an event where $E_{slowest}$ is as large as 70 GeV. We remind the reader that the neutrino spectrum falls off rather sharply in the region around 300 GeV. A close examination of Figs. 20–31 shows that most events have measured energies in reasonable agreement with the predictions of the models, but some fall outside the allowed regions. More events are required before definitive statements can be made.

In summary, none of the models are really suc-

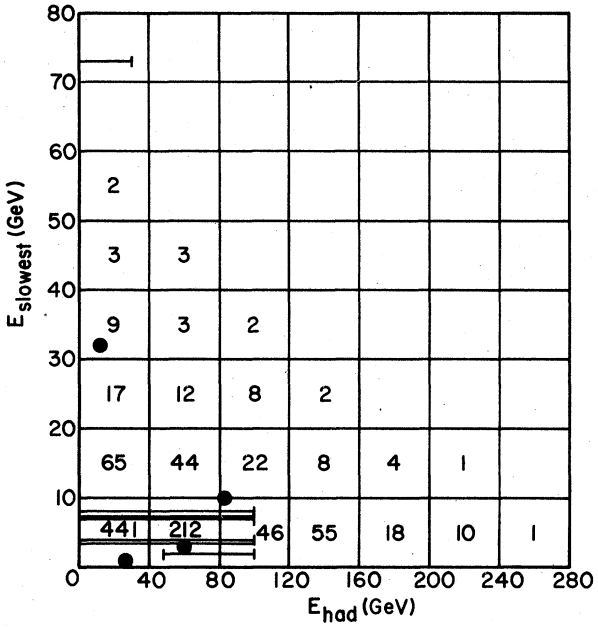


FIG. 26. Number of events in a two-dimensional scatter plot of $E_{slowest}$ versus $E_{had}$ for model A (electromagnetic production). The total number of events is normalized to approximately 1000. The dots represent the FHPRW events where $E_{had}$ is measured, and the lines represent the FHPRW events where $E_{had}$ is not measured.

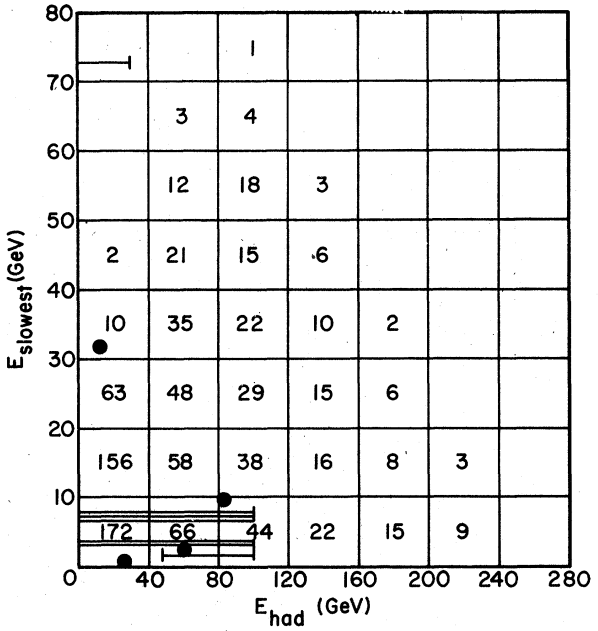


FIG. 27. Same as Fig. 26 for model B (Higgs-boson production).

cessful in explaining the two super events. Even though the angles and $p_\perp$ correlations for these events are not a problem, the energies seem anomalously large. As one can see from Figs. 20–31, the super events are completely outside the boundary of the scatter plots for some of the models. In the other cases they are very close to the edge of the scatter plot, which indicates that they occur with very low probability. If the latter models were to offer any hope of explaining the trimuon events, then many more normal events should have been detected. The models with the most favorable probability of explaining the super-events were the radiative model and the Higgs model. However, the Higgs model does not give any reasonable fit to the $M_{23}$ spectrum.

## IV. CONCLUSIONS

We have concentrated on neutrino production of trimuon events and presented single and double differential distributions to distinguish between the models A–F, namely, radiative production of muon pairs, Higgs-boson production and decay, hadron (quark) cascade, diffractive production of a pair of heavy quarks, $M^0$-hadron decays, and $M^-$ cascade decays, respectively. The distributions have been flux-averaged with the FHPRW quadrupole-triplet spectrum. The results we have given above should allow a weeding out of possible models once more data are available. The radiation of muon pairs (model A) is expected to occur with an event rate $\sigma(3\mu)/\sigma(\mu) \sim 2\times10^{-5}$ when we incorporate experimental cuts. The experimental results for $M_{23}$ already show a peaking in this vari-

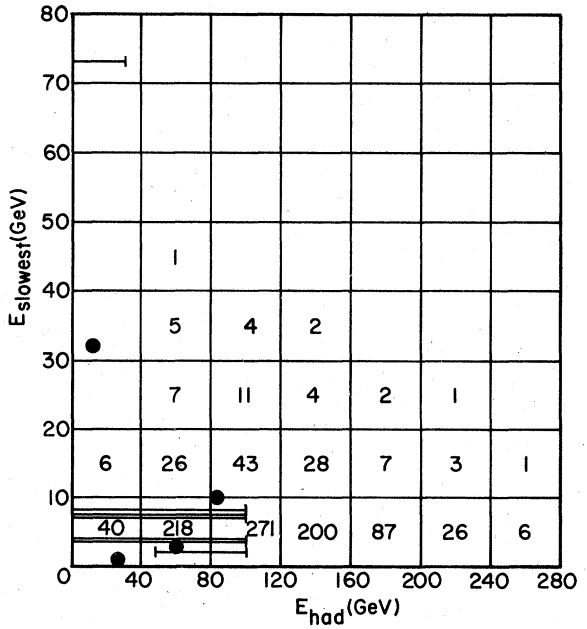


FIG. 28. Same as Fig. 26 for model C (hadron cascade).

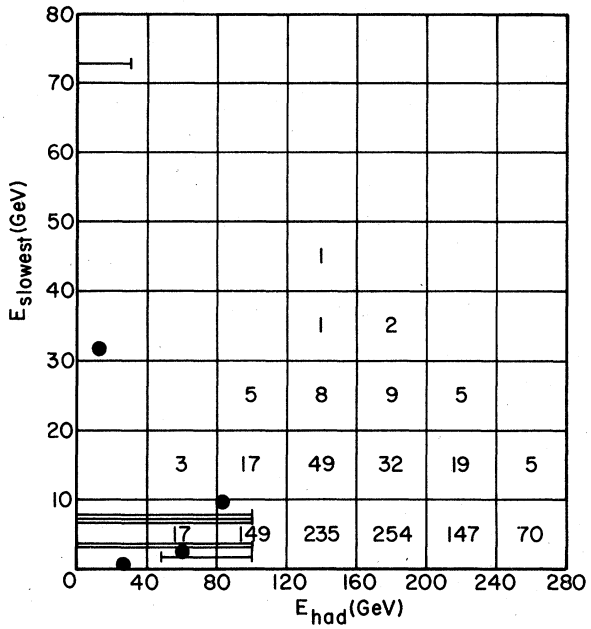


FIG. 29. Same as Fig. 26 for model D (diffractive production).

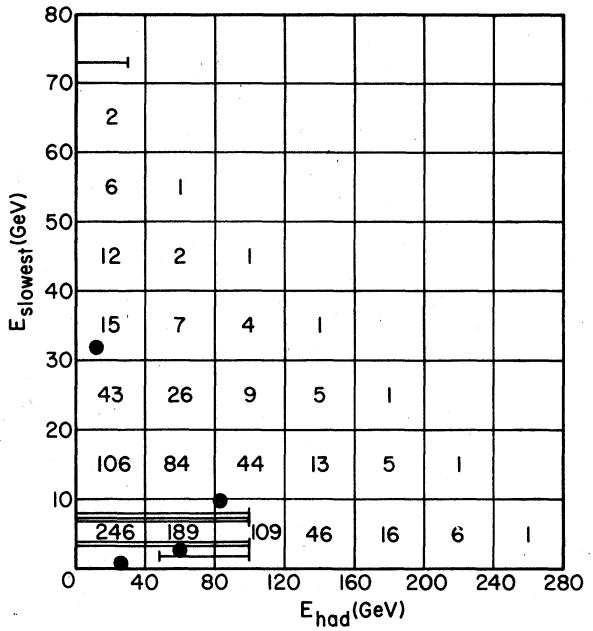


FIG. 31. Same as Fig. 26 for model F (heavy-lepton cascade).

able, and cuts can be made to remove this process. To find other signals, we see that the $M_{23}$ invariant-mass distribution is a precise test of model B, while the $M_{123}$ invariant-mass distribution will put limits on model E. The models C and D lead to spectra in $E_{\text{had}}$, which peak at large energies and cannot account for the super events which must have small $E_{\text{had}}$ energies. Heavy-lepton-cascade models, and, in particular, model F, yield muons with large transverse momenta perpendicular to the neutrino direction. The azimuthal angular distributions between pairs of muons also discriminate between leptonic- and hadronic-cascade mechanisms.

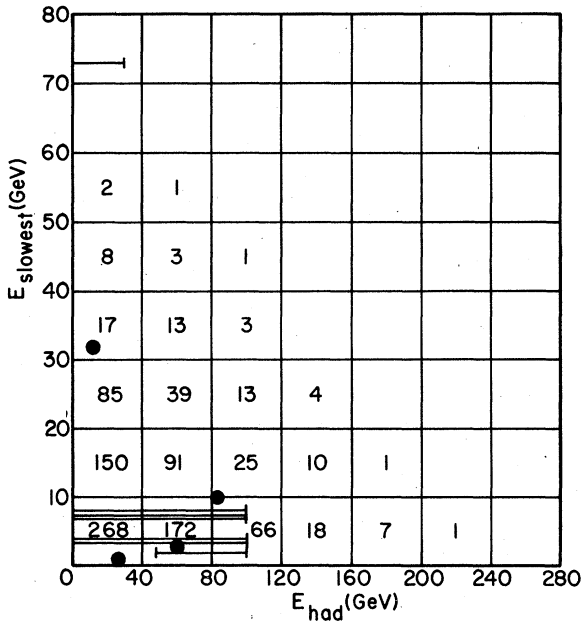


FIG. 30. Same as Fig. 26 for model E ($M^0$-hadron).

Trimuon-production rates have not been emphasized here because in general they are highly model dependent. The one exception to this rule is the electromagnetic production of muon pairs. However, even in this case, it is not clear that *all* important Feynman diagrams are included. For instance, quark-antiquark annihilation into virtual photons, which convert into muon pairs, has not been analyzed and is probably important for dimuon pairs with large invariant mass. The estimate given in Ref. 13 is certainly very reasonable, but we must remember that the predicted rate appears to be too small to account for the experimental rate, so other mechanisms are probably also present. The production cross section for model B (Higgs scalar) can be calculated reliably but it is difficult to estimate the branching ratio for $H \to \mu^+\mu^-$. While the electromagnetic production of vector mesons has been shown to be too small to fit the observed rate,[12] the hadronic production may be so large that it could account for some of the events. In that case, the $M_{23}$ invariant-mass distribution will show peaks at the position of the vector-meson masses. Both models A and B differ from the other four with respect to their $E_{\text{tot}}$ distributions. However, because there

are missing neutrinos in models C, D, E, and F, $E_{tot}$ cannot be measured accurately. The visible energy distributions may allow one to disinguish model A from other models. A careful study using a dichromatic beam can check whether the trimuon events have missing energy.

Several other tests of these models can be made using rates for the antineutrino production of $\mu^+\mu^+\mu^-$ events and neutrino/antineutrino production of same-sign dimuon and opposite-sign dimuon events. The most obvious tests involve only measurements of rates. For instance, suppose that the neutrino production of $\mu^-\mu^-$ events has a larger rate than the neutrino production of $\mu^-\mu^-\mu^+$ events. If this is true then models C, D, E, and F with new heavy leptons and/or heavy quarks will be favored because these new particles have presumably larger nonleptonic branching ratios than semileptonic branching ratios. Both the FHPRW and CDHS groups have detected $\mu^-\mu^-$ events,[2,23] but it is not a trivial problem to understand if there is a genuine signal above the background from pion and kaon decays so, unfortunately, the present situation is rather unclear. However, if the $\mu^-\mu^-$ signal turns out to be smaller than the signal for the $\mu^-\mu^-\mu^+$ events, then models which will be favored are the electromagnetic and the Higgs boson. In both cases, one should only see $\mu^-\mu^-\mu^+$, but there is a reasonably large probability that the $\mu^+$ will not survive the energy cut, so some trimuon events will be registered incorrectly as $\mu^-\mu^-$ events. The existence and magnitude of a $\mu^-\mu^-$ signal is very important and it is hoped that we will know the answer rather soon. Misidentified trimuon events of the $\mu^-\mu^+$ type will also occur but they will be very difficult to observe because of the large rate for these events arising from the production and decay of charmed particles.

The search should also be continued for opposite-sign trimuons, i.e., $\nu$-produced $\mu^-\mu^+\mu^+$ events, and for tetramuons produced in neutrino beams. The rates for these processes also impose restrictions on the possible gauge models with heavy leptons and/or heavy quarks. However, experimental acceptances and cuts have to be incorporated very carefully for such multimuon processes because the muons are so soft that events are misclassified.

The currently available antineutrino beams are much less intense than the neutrino beams, so absolute rates for trimuon production are correspondingly smaller. In the models considered above, there are important helicity effects which reduce the antineutrino cross sections relative to the neutrino cross sections. For instance, the $\bar{\nu}$ production of $\mu^+\mu^+\mu^-$ events in model A has the same rate relative to the $\bar{\nu}$ production of $\mu^+$ events as the corresponding rates for $\nu$ beams. However, the $\bar{\nu}$ cross section is reduced by the usual factor of 3 relative to the $\nu$ cross section. In terms of event rates, this factor is larger because of the absence of good $\bar{\nu}$ beams. Model D also has favorable $\bar{\nu}$ event rates because diffractively produced quark pairs have equal $\nu$ and $\bar{\nu}$ cross sections. However, models B, C, E, and F may have low $\bar{\nu}$ rates due to both the helicity effects at the production vertices and the poor $\bar{\nu}$ beams. Nevertheless, even if it were difficult to find $\bar{\nu}$-induced events, most models would prefer them to be with the charge combination $\mu^+\mu^+\mu^-$. Production of $\mu^-\mu^+\mu^+$ events in a $\nu$ beam or, alternatively, production of $\mu^+\mu^-\mu^-$ events in a $\bar{\nu}$ beam would necessitate a change in our attitude towards trimuons.

Most of the emphasis in this paper has been on the production of multimuon events because the counter experiments cannot detect electrons or positrons. However, bubble-chamber exposures should see $\mu^-e^-e^+$ events arising from model A. Searches should also be made for other exotic charge combinations such as $\mu^-\mu^+e^-$ or $\mu^-e^-$. Event rates for these reactions can be estimated for models C–F. If models A or B are correct, these signatures can only come from background processes.

*Note added.* While this paper was being prepared we received a paper from R. M. Barnett, L. N. Chang, and N. Weiss [Phys. Rev. D 17, 2266 (1978)] which also contains a comparison of different trimuon production models. We thank these authors for sending their results to us prior to publication.

## ACKNOWLEDGMENTS

This work was supported in part by the National Science Foundation under Grants Nos. Phys. 77-07864 and 76-15328 and by the Department of Energy. We would like to thank the members of the FHPRW group for discussions on their data.

---

*Permanent address: Department of Physics, Northern Illinois University, De Kalb, Illinois 60115.

[1]B. C. Barish *et al.*, Phys. Rev. Lett. 38, 577 (1977).
[2]A. Benvenuti *et al.*, Phys. Rev. Lett. 38, 1110 (1977); 40, 488 (1978); see also talk by D. Reeder, in *International Symposium on Lepton and Photon Interactions at High Energies, Hamburg, 1977,* edited by F. Gutbrod (DESY, Hamburg, 1978), p. 259.

[3]M. Holder *et al.*, Phys. Lett. 70B, 393 (1977).
[4]See reports by D. Cline and by J. Steinberger at the 1977 Irvine Meeting (unpublished).
[5]A. Benvenuti *et al.*, Phys. Rev. Lett. 38, 1183 (1977); C. H. Albright, J. Smith, and J. A. M. Vermaseren, *ibid.* 38, 1187 (1977); Phys. Rev. D 16, 3182, 3204 (1977).
[6]V. Barger, T. Gottschalk, D. V. Nanopoulos, J. Abad, and R. J. N. Phillips, Phys. Rev. Lett. 38, 1190 (1977); Phys. Rev. D 16, 2141 (1977).
[7]R. M. Barnett and L-N. Chang, Phys. Lett. 72B, 233 (1977).
[8]V. Barger, T. Gottschalk, and R. J. N. Phillips, Phys. Lett. 70B, 243 (1977).
[9]F. Bletzacker, H. T. Nieh, and A. Soni, Phys. Rev. Lett. 38, 1241 (1977); F. Bletzacker and H. T. Nieh, Stony Brook Report No. ITP-SB-77-42 (unpublished).
[10]H. Goldberg, Phys. Rev. Lett. 39, 1598 (1977). See also B-L. Young, T. F. Walsh, and T. C. Yang, Phys. Lett. 74B, 111 (1978).
[11]A. Soni, Phys. Lett. 71B, 435 (1977).
[12]R. Godbole, Phys. Rev. D 18, 95 (1978).
[13]J. Smith and J. A. M. Vermaseren, Phys. Rev. D 17, 2288 (1978).
[14]V. Barger, T. Gottschalk, and R. J. N. Phillips, Phys. Rev. D 17, 2284 (1978).
[15]P. Langacker and G. Segrè, Phys. Rev. Lett. 39, 259 (1977); P. Langacker, G. Segrè, and M. Golshani, Phys. Rev. D 17, 1402 (1978).
[15]B. W. Lee and S. Weinberg, Phys. Rev. Lett. 38, 1237 (1977). B. W. Lee and R. E. Shrock, Phys. Rev. D 17, 2410 (1978); D. Horn and G. G. Ross, Phys. Lett. 69B, 364 (1977); V. Barger, D. V. Nanopoulos, and R. J. N. Phillips, University of Wisconsin Report No. COO-597 1977 (unpublished); A. Zee, F. A. Wilczek, and S. B. Treiman, Phys. Lett. 68B, 369 (1977); S. Pakvasa, H. Sugawara, and M. Suzuki, *ibid.* 69B, 461 (1977); A. De Rújula, H. Georgi, and S. L. Glashow, Phys. Rev. D 17, 151 (1977); V. K. Cung and C. W. Kim, Phys. Lett. 69B, 359 (1977); G. C. Branco, S. Nandi, H. P. Nilles, and V. Rittenberg, Report No. BN-HY-77-9 (unpublished); J. Ellis, M. K. Gaillard, D. V. Nanopoulos, and S. Rudaz, Nucl. Phys. B131, 285 (1977). Review articles have been written by R. M. Barnett, SLAC Report No. SLAC-PUB-1961, 1977 (unpublished); and by V. Barger, University of Wisconsin Report No. COO-881-7 (unpublished).
[16]A. M. Cnops *et al.*, Phys. Rev. Lett. 40, 144 (1978).
[17]M. Perl *et al.*, Phys. Rev. Lett. 35, 1489 (1975); Phys. Lett. 63B, 466 (1976).
[18]C. H. Albright, R. E. Shrock, and J. Smith, Phys. Rev. D 17, 2383 (1978).
[19]R. Odorico, Phys. Lett. 71B, 121 (1977); R. Odorico and V. Roberto, CERN Report No. Th-2431, 1977 (unpublished).
[20]M. Suzuki, Phys. Lett. 71B, 139 (1977).
[21]J. D. Bjorken, Phys. Rev. D 17, 171 (1978).
[22]M. Holder *et al.*, Phys. Lett. 69B, 377 (1977).
[23]M. Holder *et al.*, Phys. Lett. 70B, 396 (1977).